

# Kinetics and Mechanisms of Methyl Vinyl Ketone Hydroalkoxylation Catalyzed by Palladium(II) Complexes

Kimberly J. Miller, Terutaka T. Kitagawa, and Mahdi M. Abu-Omar\*

Department of Chemistry and Biochemistry, Box 951569, 405 Hilgard Avenue,  
University of California, Los Angeles, California 90095

Received April 13, 2001

Palladium(II) coordination complexes such as  $(\text{CH}_3\text{CN})_2\text{PdCl}_2$ , **1**, catalyze the addition of alcohols to vinyl ketones to produce ethers. During the catalytic cycle, the alcohol adds selectively to the  $\beta$ -carbon (anti-Markovnikov). The kinetics for the reaction of benzyl alcohol (BA) with methyl vinyl ketone (MVK) as catalyzed by **1** has been investigated in detail. The experimental rate law is first-order in catalyst and BA and features saturation kinetics in MVK. Acetonitrile is a competitive inhibitor for MVK. The most consistent mechanism with the experimental findings involves substitution of an acetonitrile ligand by MVK in a preequilibrium step ( $K_1 = 0.020 \pm 0.004$  in  $\text{CDCl}_3$  at 25 °C) followed by nucleophilic attack of benzyl alcohol ( $k_2 = (7.6 \pm 0.8) \times 10^{-3} \text{ M}^{-1} \text{ s}^{-1}$  in  $\text{CDCl}_3$  at 25 °C). A kinetic isotope effect has been noted for the reaction in the limit of saturated MVK ( $k_2^{\text{H}}/k_2^{\text{D}} = 2.0$ ). MVK coordinates to palladium affording an  $\eta^2$ -alkene adduct. The rate constants for several alcohols are reported; the catalytic reaction is sensitive to steric hindrance of the alcohol nucleophile:  $1^\circ > 2^\circ \gg 3^\circ$ . Appreciable kinetic effects are observed by variation of the substituents on BA. Two new palladium(II) coordination complexes containing bidentate and tridentate pyridyl imine ligands have been synthesized, fully characterized, and explored as catalysts for the hydroalkoxylation reaction. The synthesis of  $\text{AgBARF}_4$  and its use in metathesis reactions with Pd(II) complexes are described. A mechanism has been put forth where the carbonyl group of the olefin interacts with palladium and directs the alcohol addition to the  $\beta$ -carbon, resulting in the anti-Markovnikov addition ether product. Finally, the charge of the palladium complex augments catalytic activity.

## 1. Introduction

Palladium-assisted addition of oxygen nucleophiles to alkenes gives a  $\sigma$ -alkyl palladium(II) intermediate which generally undergoes  $\beta$ -hydride elimination to yield aldehydes or ketones.<sup>1,2</sup> The Wacker process is the prototypical example of palladium-catalyzed oxidative hydrolysis of alkenes.<sup>3</sup> The less developed competing reaction is the protonolysis of the  $\sigma$ -alkyl bond on palladium to give the addition rather than oxidation product. When water is the nucleophile, alcohols are generated directly from alkenes (hydration).<sup>4–9</sup> Alcohols, on the other hand, produce ethers (hydroalkoxylation),<sup>10</sup> and primary amines

afford secondary amines (hydroamination).<sup>11,12</sup> Large-scale hydration of alkenes requires high acid concentrations and elevated temperatures, which limits the utility of the reaction.<sup>13,14</sup> Thus, the development of tolerant transition-metal catalysts for hydration, hydroalkoxylation,<sup>15</sup> and hydroamination<sup>16–20</sup> of olefins under mild conditions is desirable but remains challenging. Ganguly and Roundhill, for example, showed that dimeric  $\mu$ -hydroxo palladium complexes bearing bidentate phosphane ligands catalyze the hydration of diethyl maleate to diethyl malate between 120 and 140 °C;<sup>4,5</sup> however, turnover numbers were low.

\* Corresponding author. E-mail: mao@chem.ucla.edu.

- (1) Maitlis, P. *The Organic Chemistry of Palladium*; Academic Press: New York, 1971; Vol. II, pp 77–126, and references therein.
- (2) Henry, P. M. *Palladium Catalyzed Oxidation of Hydrocarbons*; D. Reidel: Dordrecht, 1980; pp 41–147.
- (3) Parshall, G. W.; Ittel, S. D. *Homogeneous Catalysis*, 2nd ed.; Wiley: New York, 1992; pp 138, and references therein.
- (4) Ganguly, S.; Roundhill, D. M. *J. Chem. Soc., Chem. Commun.* **1991**, 639–640.
- (5) Ganguly, S.; Roundhill, D. M. *Organometallics* **1993**, *12*, 4825–4832.
- (6) Stille, J. K.; James, D. E. *J. Organomet. Chem.* **1976**, *108*, 401–408.
- (7) Stille, J. K.; Divakarumi, R. *J. Organomet. Chem.* **1979**, *169*, 239–248.
- (8) Backvall, J. E.; Åkermark, B.; Ljunggren, S. O. *J. Am. Chem. Soc.* **1979**, *101*, 2411–2416.
- (9) Bennett, M. A.; Jin, H.; Li, S.; Rendina, L. M.; Willis, A. C. *J. Am. Chem. Soc.* **1995**, *117*, 8335–8340.

- (10) Hosokawa, T.; Shinohara, T.; Ooka, Y.; Murashashi, S. I. *Chem. Lett.* **1989**, 2001–2004.
- (11) Panunzi, A.; DeRenzi, A.; Palumbo, R.; Paiaro, G. *J. Am. Chem. Soc.* **1969**, *91*, 3879–3883.
- (12) Åkermark, B.; Backvall, J. E.; Hegedus, L. S.; Siirala-Hansen, K.; Sjöberg, K.; Zetterberg, K. *J. Organomet. Chem.* **1974**, *72*, 127–138.
- (13) Eguchi, K.; Tokiai, T.; Kimura, H. *Chem. Lett.* **1986**, 567–570.
- (14) Eguchi, K.; Tokiai, T.; Arai, H. *Appl. Catal.* **1987**, *34*, 275.
- (15) Lin, Y.-S.; Takeda, S.; Matsumoto, K. *Organometallics* **1999**, *18*, 4897–4899.
- (16) Dorta, R.; Egli, P.; Zurcher, F.; Togni, A. *J. Am. Chem. Soc.* **1997**, *119*, 10857–10858.
- (17) Schaffrath, H.; Keim, W. *J. Mol. Catal. A* **2001**, *168*, 9–14.
- (18) Trauthwein, H.; Tillack, A.; Beller, M. *J. Chem. Soc., Chem. Commun.* **1999**, 2029–2030.
- (19) Li, Y.; Marks, T. J. *Organometallics* **1996**, *15*, 3770–3772.
- (20) Beller, M.; Trauthwein, H.; Eichberger, M.; Breindl, C.; Mueller, T. E. *Eur. J. Inorg. Chem.* **1999**, 1121–1132.

Scheme 1

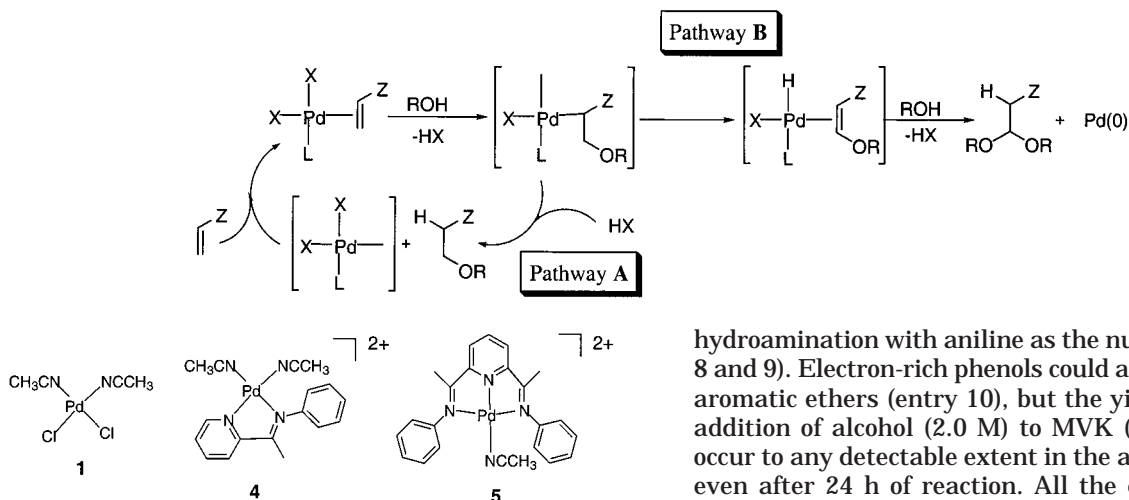


**Figure 1.** Palladium(II) coordination catalysts for hydroalkoxylation.

Addition of alcohols to a carbon–carbon double bond is a potentially useful route for making ethers from alkenes. Alcohols add to a palladium-activated  $\pi$ -complex to form a  $\sigma$ -alkyl Pd(II) intermediate, Scheme 1.  $\beta$ -Hydride migration results in the formation of a vinyl ether, which reacts readily with an additional molecule of alcohol to afford an acetal, and metallic palladium(0) is deposited (pathway B).<sup>21</sup> Alternatively, if the protonolysis of the Pd–alkyl bond is faster than  $\beta$ -hydride elimination, the result is the addition of alcohol (ROH) across the carbon–carbon double bond (pathway A).<sup>22</sup> In 1989, Hosokawa and co-workers demonstrated that pathway A with bis(acetonitrile)palladium(II) chloride is important for alkenes bearing electron-withdrawing groups (Z).<sup>10</sup>

It is worth noting that in the case of amine addition to olefins pathway A is prominent, since amines coordinate to Pd(II) more strongly than alcohols. Thus, the  $\sigma$ -alkyl intermediate is stabilized against  $\beta$ -hydride migration that causes oxidative damage.<sup>12,23,24</sup>

In this paper we report our results on the kinetics and mechanism of palladium-catalyzed hydroalkoxylation of alkenes. In addition, we now report on new palladium(II) coordination catalysts for the effective hydroalkoxylation of vinyl ketones. The catalytic reactions give regioselectively the  $\beta$ -addition product in high yields with a variety of nucleophiles. A mechanistic basis for the observed regioselectivity is presented. Additionally, we scrutinize the electronic and steric factors influencing catalysis.

## 2. Results

**2.1. Scope and Utility of the Catalytic Hydroalkoxylation Reaction.** Three monomeric palladium(II) coordination catalysts were investigated in preparative scale reactions (Figure 1). Methyl vinyl ketone (MVK) was selected as the prototypical alkene bearing an electron-withdrawing group. A variety of alcohols were reacted with MVK. Under the mild conditions employed during the reaction, the nucleophile adds to the  $\beta$ -carbon selectively. The results are summarized in Table 1. In addition, the diversity of these palladium complexes is illustrated by their ability to catalyze

hydroamination with aniline as the nucleophile (entries 8 and 9). Electron-rich phenols could also be used to give aromatic ethers (entry 10), but the yields are low. The addition of alcohol (2.0 M) to MVK (0.50 M) does not occur to any detectable extent in the absence of catalyst even after 24 h of reaction. All the employed nucleophiles afford exclusively the addition product in high yields. Neither oxidative hydroalkoxylation nor polymerization of MVK was observed. Only when the alkyl derivative of complex 4 such as  $[(\text{NN})\text{Pd}(\text{CH}_3)(\text{CH}_3\text{CN})]^+$  is employed does the polymerization of MVK ensue.<sup>25</sup>

It is worth noting that the rate of reaction is dependent on steric hindrance of the nucleophile as well as the charge of the palladium(II) complex. Both aspects will be specified via quantitative kinetics later on in the paper. With the heavier nucleophiles, the addition products were easily isolated and purified by flash chromatography. All products were fully characterized by NMR, GC/MS, and mass spectrometry. The ether products resulting from the addition of lighter alcohols to MVK were not isolated, but yields were determined by NMR and GC/MS. In most cases, the isolated yields of the addition product were comparable to reaction yields determined by NMR prior to workup (Table 1).

**2.2. Determination of the Mechanism with  $(\text{CH}_3\text{CN})_2\text{PdCl}_2$ , 1, as Catalyst. General Kinetics Experiments.** The addition of benzyl alcohol (BA) to methyl vinyl ketone (MVK) catalyzed by 1, eq 1, was chosen as a representative reaction for the initial detailed kinetic investigation. Rates of reaction were gathered via NMR, where the formation of the product and disappearance of the substrates were monitored. However, the formation of the ether product was easiest to follow because of the unique two sets of triplets in the  $^1\text{H}$  NMR spectrum at approximately 3.7 and 2.7 ppm. The two signals correspond to the two sets of hydrogens on the  $\alpha$ - and  $\beta$ -carbons with respect to the carbonyl group. All kinetic reactions were followed by NMR to completion, and 4-benzyloxy-2-butanone was the only detectable product. A representative kinetic trace is shown in Figure S1. Initial rates method was used to avoid mixed second-order kinetics during the catalytic reaction. Over prolonged periods of time, a detectable amount of palladium metal was deposited on the walls of NMR tubes. However, palladium metal does

(21) Henry, P. M. *Palladium Catalyzed Oxidation of Hydrocarbons*; D. Reidel: Dordrecht, 1980; pp 133–147.

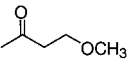
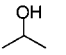
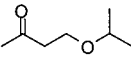
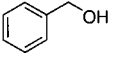
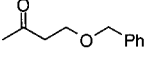
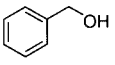
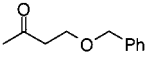
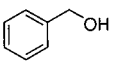
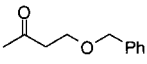
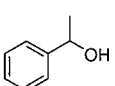
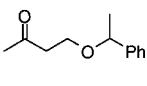
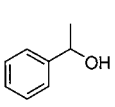
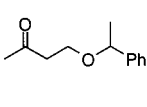
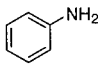
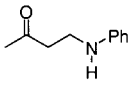
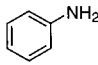
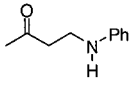
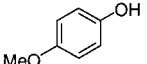
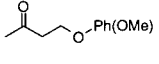
(22) Wan, W. K.; Zaw, K.; Henry, P. M. *Organometallics* **1988**, *7*, 1677–1683.

(23) Muller, T. E.; Beller, M. *Chem. Rev.* **1998**, *98*, 675–703.

(24) Kawatsura, M.; Hartwig, J. F. *J. Am. Chem. Soc.* **2000**, *122*, 9546–9547.

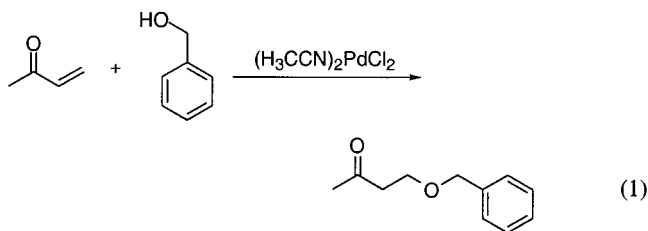
(25) Mecking, S.; Johnson, L. K.; Wang, L.; Brookhart, M. *J. Am. Chem. Soc.* **1998**, *120*, 888–899.

**Table 1. Palladium-Catalyzed Hydroalkoxylation and Hydroamination of MVK**

Entry	Nucleophile	Catalyst <sup>a</sup>	Product	% Yield <sup>b</sup> /Isolated <sup>c</sup>	TON <sup>d</sup>
1	CH <sub>3</sub> OH	<b>1</b> (Method A)		95	24 (2hr)
2		<b>1</b> (Method A)		87	22
3		<b>1</b> (Method A)		97/82	24 (72hr)
4		<b>4</b> (Method B)		97/97	97
5		<b>5</b> (Method B)		80/75	80 (6 days)
6		<b>1</b> (Method A)		76/60	19 (4 days)
7		<b>4</b> (Method B)		87/86	87
8		<b>1</b> (Method A)		90/80	23 (4 days)
9		<b>4</b> (Method B)		99/96	99
10		<b>1</b> <sup>e</sup>		49	5

<sup>a</sup> Method A: [MVK] = 1.0 mmol, [Nucleophile] = 1.0 mmol, and [**1**] = 0.040 mmol in trichloromethane ( $V_T$  = 1.0 mL) at 25 °C. Method B: [MVK] = 1.0 mmol, [Nucleophile] = 1.0 mmol, and [**4** or **5**] = 0.010 mmol in trichloromethane ( $V_T$  = 1.0 mL) at 25 °C. <sup>b</sup> Determined by <sup>1</sup>H NMR, and addition product confirmed by GC/MS. <sup>c</sup> Isolated product characterized by <sup>1</sup>H NMR and mass spectrometry. <sup>d</sup> TON = [Product]/[Pd]; all reactions were run for 48 h unless noted otherwise. In cases where more than 48 h was required, the reaction was monitored by <sup>1</sup>H NMR until product had reached a maximum. <sup>e</sup> [MVK] = 0.40 mmol, [4-methoxyphenol] = 0.80 mmol, and [**1**] = 0.040 mmol in CDCl<sub>3</sub> ( $V_T$  = 1.0 mL) at 65 °C.

not catalyze hydroalkoxylation of MVK. In the absence of catalyst, no reaction occurs even after 1 day. One limitation of the reaction was the low solubility of **1** in trichloromethane. Concentrations of **1** could not exceed 0.040 M, and stock solutions had to be used within 2 days to ensure reproducibility.



#### Determination of Reaction Orders in Substrates.

The rate of reaction was measured as a function of [MVK], while [BA] and [**1**] were held constant: [BA] = 1.0 M, [**1**] = 0.040 M, and [MVK] = 0.10–2.50 M in CDCl<sub>3</sub> at 25 °C. At low [MVK] concentrations, the rate is first-order in [MVK] but approaches zero-order at high concentrations, Figure 2. In contrast, plots of initial rate versus [BA], Figure S2, and [**1**], Figure S3, are linear.

Many reports have been published describing nucleophilic attack on ( $\eta^2$ -olefin)palladium(II) complexes.<sup>1,5,9,22,26</sup> On the basis of the current understanding in the literature and the observed kinetics in this study, we postulate the mechanism in Scheme 2. The alkene, MVK, reacts with **1** in a preequilibrium step to form an  $\eta^2$ -olefin adduct of Pd(II).<sup>22,27</sup> Benzyl alcohol, BA, then attacks the coordinated (activated) alkene to yield the ether product, regenerating the palladium catalyst. The rate law for Scheme 2, assuming steady state for the (alkene)Pd(II) complex, is given in eq 2.

$$v = -\frac{d[\text{MVK}]}{dt} = \frac{k_1 k_2 [\text{BA}][\text{MVK}][\text{Pd}]_T}{k_{-1}[\text{CH}_3\text{CN}] + k_1[\text{MVK}] + k_2[\text{BA}]} \quad (2)$$

#### Detailed Kinetics Analyses and Deciphering of Rate Constants.

To evaluate the individual rate constants, we refer to the following literature:

(26) Collman, J. P.; Hegedus, L. S.; Norton, J. R.; Finke, R. G. *Principles and Applications of Organotransition Metal Chemistry*; University Science Books: Mill Valley, CA, 1987; pp 826–841.

(27) Henry, P. M. *Palladium Catalyzed Oxidation of Hydrocarbons*; D. Reidel: Dordrecht, 1980; pp 21–25.

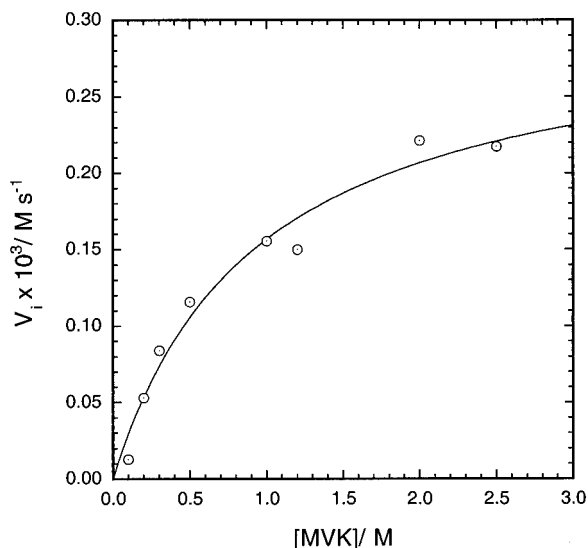


**Figure 2.** Plot of the initial rate versus [MVK] for the alkoxylation of MVK with BA catalyzed by complex **1**. The curve shows the fit of the data to the rate law in eq 3. Conditions: [BA] = 1.00 M, [**1**] = 0.040 M, and [MVK] = 0.10–2.50 M in  $\text{CDCl}_3$  at 25° C.

constants in Scheme 2, the kinetics data obtained from NMR experiments were fitted to various limits of the rate law. The observed saturation in [MVK] reduces the rate law to the prior equilibrium limit, eq 3, where  $k_1[\text{MVK}] + k_{-1}[\text{CH}_3\text{CN}] \gg k_2[\text{BA}]$ . It is worth stressing at this point that BA exhibits clean first-order dependence even at high concentrations (Figure S2). The data presented in Figure 2 was fitted to eq 3 to yield  $k_2 = (7.6 \pm 0.8) \times 10^{-3} \text{ L mol}^{-1} \text{ s}^{-1}$  in the limit of high [MVK], and  $K_1/[\text{CH}_3\text{CN}] = 1.07 \pm 0.25 \text{ L mol}^{-1}$  in the limit of low [MVK]. By fixing the value of  $K_1/[\text{CH}_3\text{CN}]$ , the slopes from the benzyl alcohol and palladium dependencies, Figures S2 and S3, furnish  $k_2 = (10 \pm 1) \times 10^{-3}$  and  $(9.9 \pm 0.7) \times 10^{-3} \text{ L mol}^{-1} \text{ s}^{-1}$ , respectively. In summary, MVK reacts with **1** in a fast step followed by the rate-determining step (RDS) in which benzyl alcohol adds to the intermediate  $(\eta^2\text{-alkene})\text{Pd}(\text{II})$  complex.

$$v = -\frac{d[\text{MVK}]}{dt} = \frac{K_1 k_2 [\text{BA}][\text{MVK}][\text{Pd}]_T}{[\text{CH}_3\text{CN}] + K_1 [\text{MVK}]} \quad (3)$$

**Inhibition Studies.** Initially, we noted that increasing the concentration of acetonitrile caused a significant decrease in the rate of reaction. Hence, we investigated the nature of the acetonitrile inhibition with respect to substrates. When MVK coordinates to the palladium catalyst, acetonitrile is most likely providing this coordination site (Scheme 2). Thus, acetonitrile would be a competitive inhibitor with respect to MVK but not BA. Rearrangement of the rate law yields the useful relationship in eq 4. The dependence of the initial rate on  $[\text{CH}_3\text{CN}]$  was probed over a range of concentrations (0.020–0.100 M) at different [MVK] (0.20, 0.40, 0.50, 0.80, and 1.00 M) but constant [**1**] (0.030 M) and [BA] (1.00 M). Plots of  $[\text{Pd}]_T[\text{BA}]/V_i$  versus  $[\text{CH}_3\text{CN}]$  are linear, with slopes that are dependent on [MVK] and have essentially common intercepts, Figure S4. The secondary plot of slopes versus  $1/[\text{MVK}]$  (Figure S4(b)) affords  $1/K_1 k_2 = (6.5 \pm 0.6) \times 10^3 \text{ M s}$  (eq 4). Since  $k_2 = 7.6 \times 10^{-3} \text{ L mol}^{-1} \text{ s}^{-1}$  from the saturation limit in

[MVK], one obtains  $K_1 = 0.020 \pm 0.004$ .

$$\frac{[\text{Pd}]_T[\text{BA}]}{V_i} = \frac{1}{K_1 k_2} \frac{[\text{CH}_3\text{CN}]}{[\text{MVK}]} + \frac{1}{k_2} \quad (4)$$

A similar study was conducted at constant [MVK] (0.50 M) and variable [BA] (0.30, 0.50, 0.80, and 1.00 M); the rate equation is specified by eq 5. Both slopes and intercepts from plots of  $[\text{Pd}]_T/V_i$  versus  $[\text{CH}_3\text{CN}]$  are linear with respect to  $1/[\text{BA}]$ , Figure S5. Thus, acetonitrile is a competitive inhibitor for MVK but not for benzyl alcohol. Furthermore, the UV-vis spectrum of the palladium complex under catalytic conditions differs from that of **1** in the limit of saturated [MVK], again, supporting “bulk” intermediate.

$$\frac{[\text{Pd}]_T}{V_i} = \frac{1}{K_1 k_2} \frac{[\text{CH}_3\text{CN}]}{[\text{MVK}][\text{BA}]} + \frac{1}{k_2} \frac{1}{[\text{BA}]} \quad (5)$$

**Kinetic Isotope Effect ( $k_2^{\text{H}}/k_2^{\text{D}}$ ).** The strength of the O–D bond is approximately 1.2 kcal/mol greater than the equivalent O–H;<sup>28</sup> thus, any effect on the rate by substituting D for H provides insight into the mechanism of hydroalkoxylation. The O–H of benzyl alcohol was exchanged to O–D (BzOD) by allowing benzyl alcohol to stir with an excess of  $\text{D}_2\text{O}$  for 2 h.  $\text{D}_2\text{O}$  was then removed by distillation, and the  $^1\text{H}$  NMR spectrum of deuterobenzyl alcohol (BzOD) was recorded to ensure complete exchange. In the saturation limit of [MVK] (Figure 2),  $k_2^{\text{BzOD}}$  was measured and found to be  $(3.8 \pm 0.4) \times 10^{-3} \text{ L mol}^{-1} \text{ s}^{-1}$ , which gives  $k_2^{\text{H}}/k_2^{\text{D}} = 2.0$ . The scission of the O–H bond is part of the RDS ( $k_2$ ).

**2.3. Kinetics with Various Alcohol Nucleophiles.** The kinetics for a number of alcohols as nucleophiles was investigated using MVK and **1**. The kinetics were followed by  $^1\text{H}$  NMR. The rates of reaction for the different alcohols were obtained by plotting the concentration of product versus time and fitting the kinetic traces to an exponential equation. The rates were then scaled relative to benzyl alcohol. Experimental conditions were as follows: [**1**] = 0.030 M, [MVK] = 0.50 M, and [ROH] = 1.00 M in  $\text{CDCl}_3$  at 25° C.  $k_2^{\text{BA}}$  was set to  $7.6 \times 10^{-3} \text{ M s}^{-1}$ , and  $k_2^{\text{ROH}}$  for other alcohols were calculated accordingly. The results for several alcohols are summarized in Table 2. Increasing the steric bulk of the nucleophile resulted in a decrease in the rate constant. A 4-fold decrease was found with both secondary alcohols,  $\alpha$ -methyl benzyl alcohol, and 2-propanol. When *tert*-butyl alcohol was employed, product yield did not exceed 5%; consequently, the reaction rate could not be determined. Cinnamyl alcohol (entry 5), an allylic alcohol, reacts slower than benzyl alcohol, in agreement with the alcohol acting as nucleophile. Conversely, methanol reacts slightly faster than benzyl alcohol. Ethyl lactate (entry 6) was chosen because of its unique H-bonding between the alcohol and carbonyl groups; thus, the breaking of the O–H bond during the hydroalkoxylation reaction could be facilitated. However, ethyl lactate was slightly slower than 2-propanol.

**2.4. Synthesis of Several Palladium(II) Coordination Complexes. Synthesis of Pyridyl Imine Palladium Complexes That Possess Two Available**

(28) Murry, J. *Organic Chemistry*, 3rd ed.; Cole Publishing Company: Pacific Grove, CA, 1992; p 394.

Scheme 2

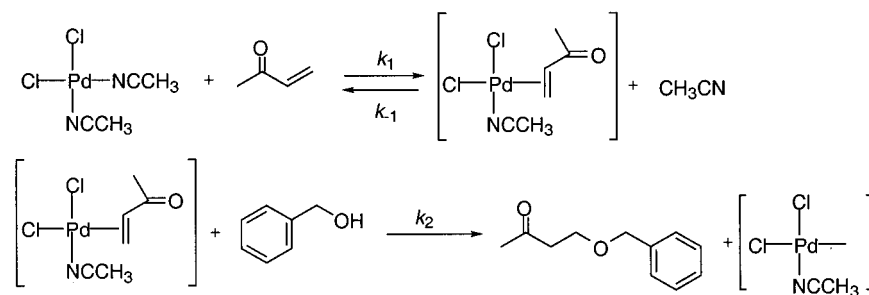


Table 2. Rate Constants for Several Alcohol Substrates.

Entry	Alcohol	$k_2$ ( $\times 10^3$ )/L mol <sup>-1</sup> s <sup>-1</sup>
1		7.6 ± 0.8
2		2.0 ± 0.2
3		1.8 ± 0.2
4	CH <sub>3</sub> OH	10 ± 1
5		1.9 ± 0.2
6		1.1 ± 0.1

**Coordination Sites.** The parent (CH<sub>3</sub>CN)<sub>2</sub>PdCl<sub>2</sub>, **1**, is a neutral species with two available coordination sites. Inhibition studies demonstrated the need for a solvent coordination site for catalytic activity, as MVK is activated by coordination to palladium. Hence, we reasoned that a coordination complex must have a solvent open coordination site, and charge should enhance the complex's Lewis acidity. Thus, we synthesized [(Py-N)-Pd(CH<sub>3</sub>CN)<sub>2</sub>][BAR<sup>F</sup><sub>4</sub>]<sub>2</sub> (Py-N = phenyl(1-pyridin-2-yl-ethylidene)amine), **4**, which contains two solvent/open coordination sites (Scheme 3). The bidentate ligand, phenyl(1-pyridin-2-yl-ethylidene)amine, was synthesized from 2,6-diacetylpyridine and aniline in a condensation reaction. The progress of the reaction was followed by monitoring the singlet at 2.70 ppm for the -CH<sub>3</sub> in the <sup>1</sup>H NMR. The ligand was then complexed to palladium to form initially the dichloride complex **2**, following a procedure by Consiglio.<sup>29</sup> The chloride ligands were metathesized with AgOTf (OTf = trifluoromethanesulfonate) to generate the dicationic compound **3** (Scheme 3).<sup>30</sup> The time required for the metathesis reaction in preparing **3** varied between 3 and 12 h depending on the AgOTf batch used. Completion of the reaction was indicated by the prominent color change from the orange-colored **2** to the yellow-colored **3**. If there is enough residual water in the solvent, the

two open coordination sites can be occupied by water molecules. Complex **3** was found to be a viable catalyst for the hydroalkoxylation reaction (eq 1); however, it is not very soluble in nonpolar solvents such as chloroform and methylene chloride. To enhance solubility, we synthesized **4** by carrying out an anion exchange with **3** and AgBAR<sup>F</sup><sub>4</sub> (BAR<sup>F</sup><sub>4</sub> = [(3,5-(CF<sub>3</sub>)<sub>2</sub>C<sub>6</sub>H<sub>3</sub>)<sub>4</sub>B]<sup>-</sup>), Scheme 3. AgBAR<sup>F</sup><sub>4</sub> was synthesized following a modified procedure of Brookhart<sup>31</sup> with AgBF<sub>4</sub> substituted in place of NaBF<sub>4</sub>. AgBAR<sup>F</sup><sub>4</sub> was utilized instead of the already known NaBAR<sup>F</sup><sub>4</sub> because the silver salt gave purer product and improved yields in comparison to the sodium salt. The disappearance of the OTf<sup>-</sup> signal at -79.92 ppm and the appearance of the BAR<sup>F</sup><sub>4</sub><sup>-</sup> signal at -63.23 ppm in the <sup>19</sup>F NMR provided direct evidence for completion of reaction. All attempts to synthesize **4** directly from **2** using AgBAR<sup>F</sup><sub>4</sub> resulted in a mixture of complexes that was difficult to separate.

**Synthesis of Pyridyl Diimine Palladium Complexes That Possess One Available Coordination Site.** In addition to complexes with two available coordination sites, we synthesized a dicationic palladium coordination complex, **5**, that contains a tridentate ligand and one open coordination site. Following the procedure of Brookhart,<sup>32</sup> we synthesized the tridentate pyridyl diimine ligand from 2,6-diacetylpyridine and aniline. <sup>1</sup>H NMR was used to check the progress of the reaction, which took a couple of days. The ligand was easily isolated by filtration because it precipitated out of solution as a yellow powder during the course of the reaction. Similar to the bidentate ligand, the six protons for the two -CH<sub>3</sub> groups show up in the <sup>1</sup>H NMR as a singlet at 2.41 ppm. The ligand was chelated to palladium following the procedure of Nesper<sup>33</sup> using the highly reactive (CH<sub>3</sub>CN)<sub>4</sub>Pd(BF<sub>4</sub>)<sub>2</sub> as the palladium starting material. An acetonitrile molecule that displays a distinct <sup>1</sup>H NMR signal at 1.96 ppm occupies the open coordination site. Following the same procedure for the preparation of **4** (Scheme 3), the BF<sub>4</sub><sup>-</sup> anion was replaced with BAR<sup>F</sup><sub>4</sub><sup>-</sup> in order to make complex **5** soluble in chloroform. The progress of the metathesis reaction was followed by <sup>19</sup>F NMR; the exclusive presence of a singlet at -63.85 ppm, which corresponds to BAR<sup>F</sup><sub>4</sub><sup>-</sup>, confirmed complete anion exchange. The full sequence of the described reactions is illustrated in Scheme 4.

(29) Sperle, M.; Consiglio, G. *J. Am. Chem. Soc.* **1995**, *117*, 12130–13136.

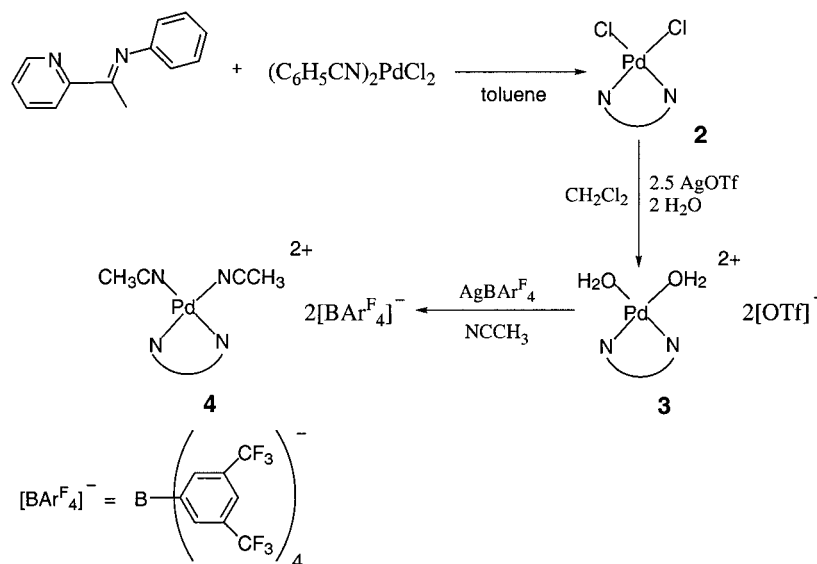
(30) Stang, P. J.; Cao, D. H.; Poulter, G. T.; Arif, A. M. *Organometallics* **1995**, *14*, 1110–1114.

(31) Brookhart, M.; Grant, B.; Volpe, A. F., Jr. *Organometallics* **1992**, *11*, 3920–3922.

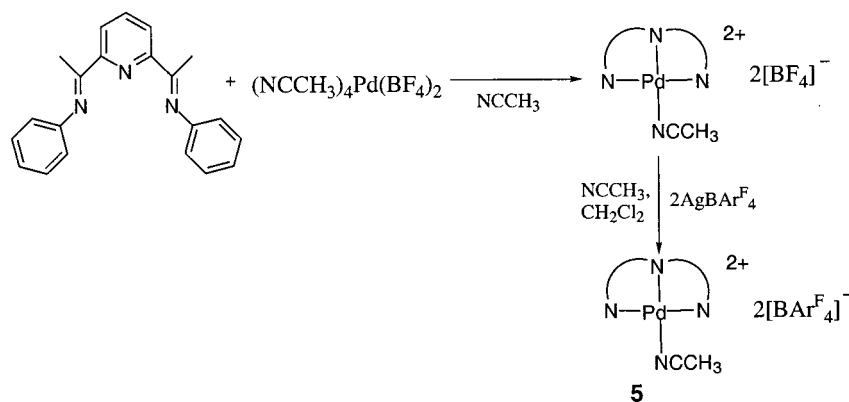
(32) Small, B. L.; Brookhart, M. *Macromolecules* **1999**, *32*, 2120–2130.

(33) Nesper, R.; Pregosin, P.; Puntener, K.; Worle, M.; Albinati, A. *J. Organomet. Chem.* **1996**, *507*, 85–101.

Scheme 3



Scheme 4



**2.5. Catalytic Activity of the New Palladium Coordination Complexes. Requirement for a Solvent Coordination Site.** The competitive inhibition by acetonitrile points toward a requirement for a coordination site that is provided by a coordinated solvent molecule. Complex **2**, (Py-N)PdCl<sub>2</sub>, is an excellent candidate to validate this hypothesis. In a reaction containing [MVK] = 0.50 M and [BA] = 1.00 M in CDCl<sub>3</sub>, 0.040 M of **2** was added, and the reaction was followed by <sup>1</sup>H NMR. No reaction was observed (0% conversion) after 24 h. After 1 day, benzyl alcohol did not coordinate in place of the chloride ligands; complex **2** was recovered unchanged. On the other hand, when complex **4** was employed as catalyst under the same conditions as those used for **2**, the reaction was completed in 90 min, yielding selectively the β-ether product.

**Kinetics and Mechanism with 4 as Catalyst.** The reaction of benzyl alcohol and MVK was used again as the model reaction for detailed kinetics. Initial rates were measured by <sup>1</sup>H NMR following the formation of the ether product. [MVK] was varied (0.10–3.0 M) at constant [4] = 0.010 M and [BA] = 1.00 M. Similar to catalyst **1**, catalyst **4** displayed saturation kinetics as the concentration of [MVK] increased, Figure 3. Therefore, the mechanism described for **1** in Scheme 2 and its corresponding prior equilibrium rate law (eq 3) apply to catalyst **4**. From the plot of initial rates

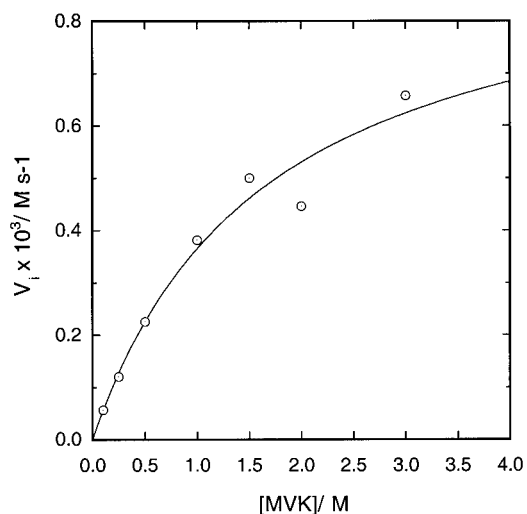


**Figure 3.** Plot of the initial rate versus [MVK] for the hydroalkoxylation of MVK with BA catalyzed by complex **4**. Conditions: [BA] = 1.00 M, [4] = 0.010 M, and [MVK] = 0.10–3.0 M in CDCl<sub>3</sub> at 25° C.

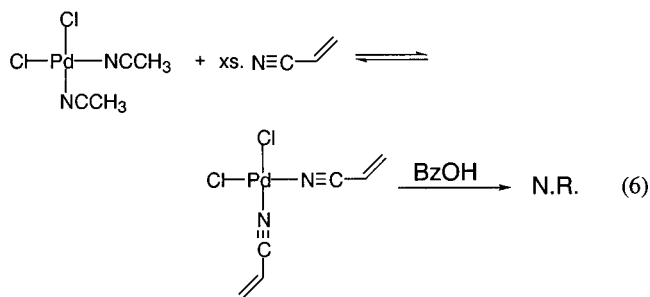
versus [MVK], one obtains  $k_2 = (97 \pm 4) \times 10^{-3} \text{ M}^{-1} \text{ s}^{-1}$  and  $K_1/[\text{CH}_3\text{CN}] = 0.61 \pm 0.05 \text{ M}^{-1}$ . Noteworthy of mention is the enhanced activity of catalyst **4** in comparison to **1**, a point that will be detailed in the Discussion.

**Tridentate versus Bidentate Ligands.** The kinetics of complex **5** were studied and compared to those of catalyst **4**. Compound **5** was found active in catalyzing the reaction of benzyl alcohol with MVK. However, the rate of reaction catalyzed by **5** is 69 times slower than that catalyzed by **4**,  $k_2(\mathbf{5}) = (1.4 \pm 0.1) \times 10^{-3} \text{ M}^{-1} \text{ s}^{-1}$ . Nevertheless, given enough time, the addition of benzyl alcohol to MVK proceeded in excess of 90% conversion with high regioselectivity in favor of the  $\beta$ -product. Typical conditions for reactions with **5** were as follows: [MVK] = 0.50 M, [BA] = 1.00 M, and [5] = 0.0060 M in  $\text{CDCl}_3$  at 25° C.

### 3. Discussion

We have shown from the experimentally determined rate law in eq 3 that the catalytic reaction (eq 1) is a two-substrate system in its kinetics as well as in its chemistry. Saturation kinetics in one of the substrates, MVK, has been observed. The mechanism in which MVK coordinates to palladium in place of an acetonitrile (Scheme 2) is supported on the basis of the following: (1) Acetonitrile is a competitive inhibitor with respect to MVK, while chloride is uncompetitive. (2) The RDS in the limit of saturated MVK features a significant kinetic isotope effect,  $k_2^{\text{H}}/k_2^{\text{D}} = 2.0$ . (3) Acetonitrile is a noncompetitive inhibitor for BA. (4) A catalyst that lacks an available/solvent coordination site such as complex **2** is totally inactive. (5) Complex **2** does not undergo a substitution reaction with benzyl alcohol even after 1 day.

Even though MVK may coordinate to palladium through the alkene or the carbonyl's oxygen,  $\eta^2$ -olefin complexes of palladium(II) are highly precedent.<sup>27,34</sup> To scrutinize the mode of MVK coordination in our system, we studied the activity of acrylonitrile, which is analogous to MVK.<sup>35</sup> While acrylonitrile coordinated to complex **1** through the nitrogen, eq 6, it did not react with benzyl alcohol (no detectable product even after 1 day). Furthermore,  $\sigma$ -alkyl palladium(II) coordination complexes have been shown to catalyze the copolymerization of methyl acrylate and ethylene.<sup>36</sup> Their ability to tolerate the carbonyl functional group implied that coordination via the carbonyl's oxygen is not favored over olefin binding. Indeed, this would be the case here as well.

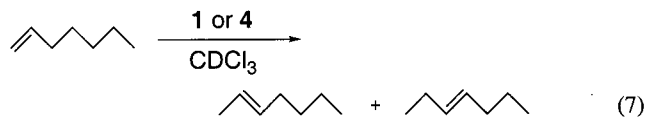


As for unfunctionalized terminal alkenes, they did not undergo hydroalkoxylation. For example, styrene does

(34) Fujii, A.; Hagiwara, E.; Sodeoka, M. *J. Am. Chem. Soc.* **1999**, *121*, 5450–5458.

(35) Typical conditions were [1] = 0.040 M, [BA] = 1.00 M, and [H<sub>2</sub>C=CHCN] = 0.50 M in  $\text{CD}_2\text{Cl}_2$  at 25 °C.

not react with BA, and 1-heptene isomerizes instead to 2- and 3-heptene, eq 7.<sup>37</sup> Isomerization of 1-heptene took ~2 min to reach completion when catalyzed by complex **4** and ~10 min with **1** as catalyst. More importantly, BA did not inhibit the reaction, indicating that the alcohol either weakly coordinates (labile) or does not coordinate to the palladium.



Once the ( $\eta^2$ -MVK)Pd(II) adduct is formed, external attack of the alcohol (nucleophile) from outside the coordination sphere of palladium(II) affords a ( $\sigma$ -alkyl)-Pd(II) intermediate. Several studies on the analogous palladium-catalyzed hydration reaction are germane to the present study. On the basis of stereochemical results, hydroxypalladation (addition of water to a coordinated olefin) was believed to occur by external attack of water.<sup>6–8</sup> However, other studies on aqueous olefin oxidation and platinum(II) model complexes support olefin insertion into an M–OH(R) bond.<sup>5,9,22,38,39</sup> Details of the hydroxypalladation mechanism are still being debated.<sup>3</sup> Nevertheless, in the present hydroalkoxylation study, the results are in favor of a trans nucleophilic attack. The RDS displays a significant kinetic isotope effect on the alcohol's O–H(D) group. It is unlikely that deprotonation of a coordinated alcohol is rate-controlling. Also, catalyst **5**, which has only one available coordination site, is active in hydroalkoxylation of MVK. However, the slow kinetics displayed by **5** in comparison to **4** can be attributed to either sterics or arm-opening of the tridentate ligand to give bidentate coordination.<sup>40</sup> The latter scenario is precluded, since the <sup>1</sup>H NMR spectrum of **5** is symmetric at room temperature and the kinetics are dependent on the substrate's concentration. If the much lower rate observed with **5** is due to ligand dissociation, the kinetics would be zero order in substrates.

We turn next to regioselectivity. During the catalytic cycle, the carbonyl group most likely interacts with palladium, thus acting as a directing group.  $\eta^2$ -Coordination of an alkene to a transition metal results in the activation of both carbons, and nucleophilic attack is usually favored for the more substituted olefinic carbon.<sup>1,41,42</sup> However, the carbonyl interaction with palladium would generate a partial positive charge on the  $\beta$ -carbon, making it more susceptible toward nucleophilic attack, eq 8. In the final step, protonolysis of the  $\sigma$ -alkyl bond affords the ether product and regenerates the catalyst.

(36) Johnson, L. K.; Mecking, S.; Brookhart, M. *J. Am. Chem. Soc.* **1996**, *118*, 267–268.

(37) Conditions: 1-heptene = 0.50 M, benzyl alcohol = 1.00 M with **1** = 0.040 M or **4** = 0.010 M as catalyst in  $\text{CDCl}_3$  at 25 °C.

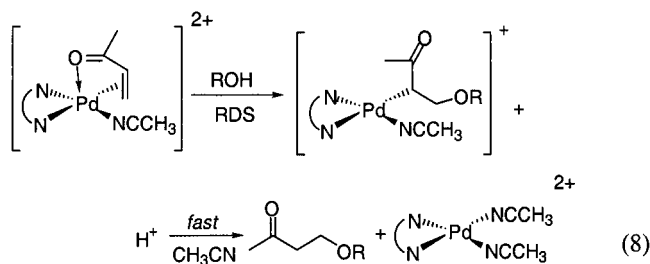
(38) Gregor, N.; Zaw, K.; Henry, P. M. *Organometallics* **1984**, *3*, 1251–1256.

(39) Bryndza, H. E. *Organometallics* **1985**, *4*, 406–408.

(40) Rulke, R. E.; Han, I. M.; Elsevier, C. J.; Vrieze, K.; van Leeuwen, P. W. N. M.; Roobeek, C. F.; Zoutberg, M. C.; Wang, Y. F.; Stam, C. H. *Inorg. Chim. Acta* **1990**, *169*, 5–8.

(41) Hartley, J. F. *Nature* **1969**, *223*, 615–616.

(42) Hartley, F. R. *Chemistry of Platinum and Palladium*; John Wiley & Sons: New York, 1973; p 384.



Under conditions employed in this investigation, acetals resulting from vinyl ether oxidation products (Scheme 1) are not detected. The  $\sigma$ -alkyl palladium(II) intermediates must be stabilized with respect to  $\beta$ -hydrogen migration, or the protonolysis of the Pd–alkyl bond is much faster than the competing  $\beta$ -hydrogen elimination. Certainly a vacant or weakly coordinated site that is cis to the Pd–alkyl bond is required for oxidative decomposition.<sup>43</sup> Such a site is not present in catalyst **5**, accounting for the stability of **5** under catalytic conditions for prolonged periods of time (entry 5 in Table 1). Catalyst **4** is not only more reactive than catalyst **1** but also more stable in solution. The acetonitrile ligand of **4** is more tightly bound, and its dissociation is slow on the time scale of the protonolysis reaction. Even complex **1** is reasonably stable toward oxidative decomposition; this is evident by the high yields of hydroalkoxylation product (Table 1). An additional factor in stabilizing the  $\sigma$ -alkyl palladium(II) intermediate could very well be the carbonyl group on MVK. Its interaction with palladium would hinder  $\beta$ -hydride elimination, thus favoring the formation of the ether product.<sup>44</sup>

The structure–function correlation of Hammett<sup>45–47</sup> accounts for various reactions of *meta*- and *para*-substituted aromatic compounds. Benzyl alcohol substrates with different substituents on the *para* positions were examined. Values for  $\sigma_p$  are listed in Table 3 alongside the  $\log(k_X/k_H)$  values for the different benzyl alcohols with both catalysts **1** and **4**. Figure S6 shows two plots of  $\log(k_X/k_H)$  versus  $\sigma_p$  for catalysts **1** and **4**. The slopes afford the reaction constants for both catalysts,  $\rho(\mathbf{1}) = -0.63 \pm 0.07$  and  $\rho(\mathbf{4}) = -0.70 \pm 0.13$ . The linear Hammett correlation suggested that all the benzyl alcohols react by the same mechanism in each of the catalytic systems. The negative sign of  $\rho$  is in agreement with nucleophilic attack of the alcohol on the electrophilically activated MVK. Thus, a positive charge buildup on oxygen characterizes the transition state. The identical reaction constants ( $\rho$ ) for **1** and **4** indicate a common mechanism for both catalysts.

The effect of charge on catalytic activity deserves a comment. Catalyst **4** is 13 times more reactive than **1**. The dicationic charge of complex **4** results in a stronger Lewis acid and thus is more reactive compared to the neutral complex **1**. Although the pyridine ligand in **4** is a  $\pi$ -acceptor, its contribution to the Lewis acidity of **4**

**Table 3. Substituent Effects on the Rate Constants for Substituted Benzyl Alcohols with Catalysts **1** and **4**<sup>a</sup>**

Alcohol	$\sigma_p$	$\log(k_X/k_H)$	
		Cat. <b>1</b>	Cat. <b>4</b>
	-0.17	0.056	-0.15
	0.00	0.00	0.00
	0.23	-0.063	-0.19
	0.45	-0.29	—
	0.54	-0.38	-0.41

<sup>a</sup> In  $\text{CDCl}_3$  at 25 °C.

**Table 4. Comparison of the Relative Rates for the Different Catalysts Used in This Study<sup>a</sup>**

catalyst	no. of open coord sites	charge	rel rate <sup>b</sup>
$(\text{CH}_3\text{CN})_2\text{PdCl}_2$ , <b>1</b>	2	0	1.0
$(\text{Py-N})\text{PdCl}_2$ , <b>2</b>	0	0	n.r. <sup>c</sup>
$[(\text{Py-N})\text{Pd}(\text{CH}_3\text{CN})_2][\text{BAR}^F_4]_2$ , <b>4</b>	2	+2	13
$[(\text{N-Py-N})\text{Pd}(\text{CH}_3\text{CN})][\text{BAR}^F_4]_2$ , <b>5</b>	1	+2	0.19

<sup>a</sup> The reaction used is the hydroalkoxylation of MVK with benzyl alcohol (eq 1). <sup>b</sup> Determined by comparing  $k_2$  values for each catalyst. <sup>c</sup> n.r. = no reaction.

would be minor in comparison to the effect of charge. Table 4 compares the reactivities of the different catalysts from this study as a function of charge and available (solvent) coordination sites.

#### 4. Summary

Via kinetics studies and substrate probes, the mechanism of palladium(II)-catalyzed hydroalkoxylation of vinyl ketones has been defined. At least one coordination site on palladium must be available. The vinyl ketone is activated via  $\eta^2$ -coordination of the alkene to palladium(II); the alcohol nucleophile attacks selectively the  $\beta$ -carbon of the  $\pi$ -olefin adduct. Saturation kinetics are observed for MVK, and deuterio-alcohols (ROD) display a primary kinetic isotope effect,  $k_H/k_D = 2.0$ , which implies O–H bond breaking in the transition state. The observed regioselectivity is rationalized by invoking an interaction between the carbonyl group and palladium. Charge on the palladium catalyst enhances its Lewis acidity and boosts activity. On the basis of the mechanistic information described here, we are currently extending this catalytic reaction to asymmetric hydroalkoxylation and kinetic resolution of racemic alcohols.

#### 5. Experimental Section

**Materials and Instrumentation.** All chemicals were obtained commercially. The bis(acetonitrile) dichloropalladium(II) was a gift from Alfa Aesar. Acetonitrile, benzene, and methylene chloride were dried over calcium hydride. Toluene was dried and stored over molecular sieves. All reactions were

(43) Winstein, S. W.; McCaskie, J.; Lee, H.-B.; Henry, P. M. *J. Am. Chem. Soc.* **1976**, *98*, 6913–6918.

(44) Zuideveld, M. A.; Kamer, P. C. J.; van Leeuwen, P. W. N. M.; Klusener, P. A. A.; Stil, H. A.; Roobeek, C. F. *J. Am. Chem. Soc.* **1998**, *120*, 7977–7978.

(45) Hammett, L. P. *Chem. Rev.* **1935**, *17*, 125.

(46) Hammett, L. P. *Physical Organic Chemistry*; McGraw-Hill Book Co.: New York, 1940; pp 184–228.

(47) Hansch, A.; Leo, T. R. *Chem. Rev.* **1991**, *91*, 165–195.



carried out in dried glassware and under argon unless noted otherwise. However, all complexes were fairly stable toward air, moisture, and light. NMR spectra were collected on a Bruker 200 MHz and/or 400 MHz spectrometers. GC/MS experiments were conducted on a Hewlett-Packard G1800A GCD system equipped with an HP-5MS capillary column packed with cross-linked 5% PH ME siloxane; a temperature program was employed in all GC/MS runs: 80–140 °C at 7 °C/min, then 140–220 °C at 10 °C/min. Elemental analyses were done in duplicates by Desert Analytics, AZ.

**Kinetics Studies.** An NMR tube was charged via syringe with the desired concentrations of MVK and alcohol. The total volume was brought to 1.0 mL with CDCl<sub>3</sub>. TMS (0.08 mmol) was added as an internal standard. The desired amount of catalyst was weighed on an analytical balance and added last to the assay mixture. The reaction was monitored by <sup>1</sup>H NMR on a Bruker ARX 400 MHz spectrometer at 25 °C. Initial rates were evaluated for the first 10% of reaction. All kinetic runs proceeded to completion. Product concentrations were determined by integration of the carbonyl –CH<sub>3</sub> signal of the ether product versus MVK or TMS. When MVK was used in excess to BA, the –CH<sub>2</sub> signal of the benzyl alcohol was used. The initial rate for each run was the average of duplicates. For the inhibition studies, acetonitrile was added from a stock solution of acetonitrile (1.0 M) in CD<sub>3</sub>Cl.

**A Typical Catalytic Hydroalkoxylation Procedure.** To 1.0 mmol of methyl vinyl ketone was added 1.0 mmol of ROH or PhNH<sub>2</sub>, and the mixture was diluted in deuteriochloroform (V<sub>T</sub> = 1.0 mL). The reaction was initiated by addition of the palladium catalyst (**1** = 40 μmol, **4** or **5** = 10 μmol). The progress of reaction was followed by <sup>1</sup>H NMR until no more product was being formed. The reaction solution was passed through a silica plug (6.0 × 0.5 cm) with diethyl ether (~5 mL) as eluent. The catalyst-free colorless solution was collected, and the solvent was removed under vacuum. If the eluted solution remained colored after the initial silica plug, it was filtered again through a second silica plug. The isolated products were fully characterized by <sup>1</sup>H NMR, GC/MS, and FAB<sup>+</sup>-MS. The spectroscopic data for all of the products in Table 1 follow.

**4-Methoxy-2-butanone.** <sup>1</sup>H NMR (CD<sub>3</sub>Cl): δ 3.54 (t, 2H), 3.22 (s, 3H), 2.57 (t, 2H), 2.09 (s, 3H). GC/MS: *t*<sub>R</sub> = 2.01 min.

**4-(2-Propoxy)-2-butanone.** <sup>1</sup>H NMR (CD<sub>3</sub>Cl): δ 3.54 (sept, 1H), 3.48 (t, 2H), 2.63 (t, 2H), 2.15 (s, 3H), 1.13 (d, 6H). GC/MS: *t*<sub>R</sub> = 2.95 min.

**4-Benzoyloxy-2-butanone.** <sup>1</sup>H NMR (CD<sub>3</sub>Cl): δ 7.24 (m, 6H), 4.44 (s, 2H), 3.66 (t, 2H), 2.61 (t, 2H), 2.10 (s, 3H). FAB<sup>+</sup>/MS: *m/z* 179 (M + H)<sup>+</sup>, 177 (M – H)<sup>+</sup>. GC/MS: *t*<sub>R</sub> = 12.11 min.

**4-(2-sec-Phenylethoxy)butanone.** <sup>1</sup>H NMR (CD<sub>3</sub>Cl): δ 7.24 (m, 6H), 4.31 (q, 1H), 3.45 (t, 2H), 2.55 (t, 2H), 2.08 (s, 3H), 1.32 (d, 3H). FAB<sup>+</sup>/MS: *m/z* 191 (M + H)<sup>+</sup>, 192 (M<sup>+</sup>), 193 (M – H)<sup>+</sup>. GC/MS: *t*<sub>R</sub> = 11.94 min.

**4-(N-Phenylamino)-2-butanone.** <sup>1</sup>H NMR (CD<sub>3</sub>Cl): δ 7.12 (m, 2H), 6.69 (m, 4H), 3.40 (t, 2H), 2.73 (t, 2H), 2.14 (s, 4H). FAB<sup>+</sup>/MS: *m/z* 163 (M<sup>+</sup>). GC/MS = *t*<sub>R</sub> = 12.89 min.

**4-(p-Methoxyphenoxy)-2-butanone.** <sup>1</sup>H NMR (CD<sub>3</sub>Cl): δ 6.95 (s, 4H), 4.17 (t, 2H), 3.86 (s, 3H), 2.88 (t, 2H), 1.96 (s, 3H). GC/MS: *t*<sub>R</sub> = 13.71 min.

**Synthesis of Phenyl(1-pyridin-2-ylethylidene)amine (Py-N).** To a flask with a Dean–Stark trap was added 2-acetylpyridine (2.0 mL, 17.83 mmol), aniline (9.0 mL, 98.8 mmol), 7 drops of 88% formic acid, and 30 mL of benzene. The trap was filled with benzene, and the solution was refluxed until ~0.3 mL of water was collected. The reaction solution was then cooled to room temperature and the excess aniline removed under vacuum at ~90 °C, to remove the excess aniline completely. The ligand product was a dark red oil but yellow in solution. Yield = 44%. <sup>1</sup>H NMR (CD<sub>2</sub>Cl<sub>2</sub>): δ 8.55 (d, 1H), 8.17 (d, 1H), 7.71 (t, 1H), 7.26 (t, 3H), 7.05 (t, 1H), 6.73 (d, 2H), 2.70 (s, 3H).

**Synthesis of [Phenyl(1-pyridin-2-ylethylidene)amine]-PdCl<sub>2</sub>, **2**.** In a two-neck round-bottom flask, benzylnitrilepalladium(II) chloride (0.10–1.0 g) was dissolved in 150 mL of toluene. The solution was heated to 70 °C. One equivalent of the ligand was added dropwise via an addition funnel. After the addition was completed, the solution was stirred at 70 °C for 2.5 h. During the addition, the solution changed color from dark orange to yellow. The reaction was cooled to room temperature, after which 200 mL of pentane was added. The precipitated product was isolated by filtration and washed with 50 mL of ether. The isolated product was a yellow solid and was stable to air and moisture. Yield = 89%. <sup>1</sup>H NMR (CD<sub>2</sub>-Cl<sub>2</sub>): δ 9.43 (d, 1H), 8.21 (t, 1H), 7.91 (d, 1H), 7.65 (t, 1H), 7.46 (m, 3H), 7.10 (d, 2H), 2.31 (s, 3H). FAB<sup>+</sup>/MS: *m/z* 373.6 (M<sup>+</sup> ion; correct isotope distribution for Pd). Anal. Calcd 41.80 C, 3.24 H, 7.50 N, 18.98 Cl. Found: 42.10 C, 3.12 H, 7.23 N, 17.83 Cl.

**Synthesis of [Phenyl(1-pyridin-2-ylethylidene)amine]-Pd(H<sub>2</sub>O)<sub>2</sub>·2OTf, **3**.** In a 50 mL three-neck flask, **2** (0.10 g, 0.27 mmol) was dissolved in 30 mL of CH<sub>2</sub>Cl<sub>2</sub>. After most of the starting material had dissolved, 2.5 equiv of AgOTf was added. The heterogeneous solution was protected from light and stirred until the solution turned yellow. The amount of time fluctuated between 3 and 12 h depending on how pure and dry the silver triflate was. The solution was then filtered through a glass frit to remove the AgCl and any unreacted AgOTf. The solid was washed with 20 mL of dry acetonitrile. The combined filtrate was placed under vacuum until a dry solid was obtained. The resulting yellow product needed no further purification. Because the product decomposes with time, the solid was stored in the glovebox. Yield = 72%. <sup>1</sup>H NMR (CD<sub>3</sub>CN): δ 8.52 (d, 1H), 8.46 (t, 1H), 8.15 (d, 1H), 7.89 (t, 1H), 7.56 (m, 3H), 7.33 (d, 2H), 2.40 (s, 3H), 2.12–2.09 (s, 4H). <sup>19</sup>F NMR (CD<sub>3</sub>CN): δ –79.92. FAB<sup>+</sup>/MS: *m/z* 451.0 (–2H<sub>2</sub>O, OTf<sup>–</sup>), 301.9 (–2H<sub>2</sub>O, 2OTf<sup>–</sup>) (M<sup>+</sup> ion; correct isotope for Pd). Anal. Calcd 28.29 C, 2.53 H, 4.40 N, 10.07 S. Found: 30.42 C, 2.79 H, 4.36 N, 9.96 S.

**Synthesis of [Ag][(3,5-(CF<sub>3</sub>)<sub>2</sub>C<sub>6</sub>H<sub>3</sub>)<sub>4</sub>B] (AgBAR<sup>F</sup><sub>4</sub>).** In a three-neck round-bottom flask equipped with an addition funnel, 1.28 g (52.5 mol) of Mg turnings were stirred in 32 mL of ether. 3,5-Bis(trifluoromethyl)bromobenzene, 7.3 mL (42.5 mol), was diluted in 62.5 mL of ether and then added to the three-neck flask via addition funnel at room temperature. After the addition was completed, the solution was heated to reflux for 30 min, resulting in a dark brown solution. The reaction was cooled to room temperature, and 1.47 g (7.5 mmol) of AgBF<sub>4</sub> was added. This solution was stirred for 60 h. In a separate flask, a solution containing 18.75 g of Na<sub>2</sub>CO<sub>3</sub> in 250 mL of water was prepared. The reaction mixture was poured into the Na<sub>2</sub>CO<sub>3</sub> solution and filtered. The aqueous layer was separated and extracted with 4 × 100 mL of ether. The ether extracts were combined, and the solvent was removed. The resulting brown solid was washed with ~5 mL of cold CH<sub>2</sub>Cl<sub>2</sub> and dried under vacuum. The product was isolated as a tan solid. Yield = 41%. <sup>1</sup>H NMR (CD<sub>2</sub>Cl<sub>2</sub>): δ 8.01 (s, 8H), 7.86 (s, 4H). <sup>19</sup>F NMR (CD<sub>2</sub>Cl<sub>2</sub>): δ –63.4. <sup>11</sup>B NMR (CH<sub>2</sub>Cl<sub>2</sub>): δ –6.67. FAB<sup>–</sup>/MS: *m/z* 863.07 (M<sup>–</sup> ion; correct isotope for B).

**Synthesis of [(Phenyl(1-pyridin-2-ylethylidene)amine)-Pd(CH<sub>3</sub>CN)<sub>2</sub>][BAR<sup>F</sup><sub>4</sub>]<sub>2</sub>, **4**.** Both **3** and AgBAR<sup>F</sup><sub>4</sub> were placed in a Schlenk flask and dissolved in 10 mL of dry CH<sub>3</sub>CN. The solution was stirred for 2 h, at which time the solution had turned a dark orange color. The solvent was removed under vacuum. The isolated solid was redissolved in CH<sub>2</sub>Cl<sub>2</sub>. The AgOTf byproduct did not dissolve and was separated by cannulation. The solvent was removed under vacuum to give a pure yellow solid. Yield = 69%. <sup>1</sup>H NMR (CD<sub>2</sub>Cl<sub>2</sub>): δ 8.43 (t, 1H), 8.23 (d, 1H), 8.04 (d, 1H), 7.34 (t, 1H), 7.72 (s, 16H), 7.60 (t, 3H), 7.56 (s, 8H), 7.20 (m, 2H), 2.48 (s, 6H), 1.93 (br s, 6H). <sup>19</sup>F NMR (CD<sub>3</sub>CN): δ –63.37. FAB<sup>+</sup>/MS: *m/z* 302.00 (–2H<sub>2</sub>O) (M<sup>+</sup> ion; correct isotope for Pd). Anal. Calcd 45.52 C, 2.01 H, 2.65 N, 43.18 F. Found: 41.47 C, 1.82 H, 2.29 N, 39.59 F.

**Synthesis of 2,6-Bis[1-ethylphenylimino]pyridine (N-Py-N).** In a round-bottom flask, 2,6-diacetylpyridine (1.0 g, 6.13 mmol) and an excess of aniline (5.6 mL, 61.5 mmol) were dissolved in 50 mL of absolute EtOH. Seven drops of 88% formic acid were added. The flask was sealed and stirred at room temperature for 4 days. During this time, a bright yellow precipitate began to form. The progress of the reaction was followed by  $^1\text{H}$  NMR. Once conversion was above  $\sim 55\%$ , the solution was filtered and a bright yellow solid was recovered. Yield = 59%.  $^1\text{H}$  NMR ( $\text{CD}_3\text{Cl}$ ):  $\delta$  8.36 (d, 2H), 7.89 (t, 1H), 7.37 (t, 4H), 7.13 (t, 2H), 6.86 (d, 4H), 2.41 (s, 6H).

**Synthesis of 2,6-Bis[1-ethylphenylimino]pyridinePd(NCCH<sub>3</sub>)<sub>2</sub>·2BF<sub>4</sub>.** ( $\text{NCCH}_3$ )<sub>4</sub>Pd(BF<sub>4</sub>)<sub>2</sub> (0.0840 g, 0.13 mmol) and 0.0597 g (0.19 mmol) of 2,6-bis[1-ethylphenylimino]pyridine ligand were dissolved in 5 mL of acetonitrile. The reaction was protected from light, and the solution was stirred at room temperature for 20 min. The solvent was then removed to give the yellow (N-Py-N)Pd(CH<sub>3</sub>CN)·2BF<sub>4</sub> product. Yield = 95%.  $^1\text{H}$  NMR ( $\text{CD}_2\text{Cl}_2$ ):  $\delta$  8.60 (t, 1H), 8.18 (d, 2H), 7.48 (t, 4H), 7.46 (t, 2H), 7.28 (d, 4H), 2.48 (s, 6H), 1.96 (s, 3H).  $^{19}\text{F}$  NMR ( $\text{CD}_3\text{CN}$ ):  $\delta$  -152.18.

**Synthesis of 2,6-Bis[1-ethylphenylimino]pyridinePd(NCCH<sub>3</sub>)<sub>2</sub>·2BAr<sup>F</sup>, 5.** (N-Py-N)Pd(CH<sub>3</sub>CN)·2BF<sub>4</sub> (0.0787 g, 0.12 mmol) was dissolved in 5 mL of acetonitrile, and 0.2490 g (0.25 mmol) of AgBAr<sup>F</sup> was added in one portion. The reaction

mixture was stirred at room temperature for 2 h. The solvent was removed under vacuum, and 5 mL of dry  $\text{CH}_2\text{Cl}_2$  was added to the product mixture. The insoluble byproduct ( $\text{AgBF}_4$ ) was separated via cannulation. Methylene chloride was removed from the filtrate, and the resulting yellow product was dried in a vacuum. Yield = 91%.  $^1\text{H}$  NMR ( $\text{CD}_2\text{Cl}_2$ ):  $\delta$  8.60 (t, 1H), 8.18 (d, 2H), 7.67 (s, 16H), 7.57 (s, 8H), 7.54 (t, 4H), 7.46 (t, 2H), 7.28 (d, 4H), 2.48 (s, 6H), 1.96 (s, 3H).  $^{19}\text{F}$  NMR ( $\text{CD}_3\text{CN}$ ):  $\delta$  -63.85.

**Acknowledgment.** This research was supported by the National Science Foundation (CHE-9874857-CA-REER) and the Arnold and Mabel Beckman Foundation through a BYI to M.M.A.O. We are grateful to Mr. Lee McPherson for the experiments with acrylonitrile.

**Supporting Information Available:** A representative kinetic trace (Figure S1), plots of  $V_i$  versus [BA] and [1] (Figures S2 and S3), kinetic plots as well as secondary plots for acetonitrile inhibition studies (Figures S4 and S5), and Hammett plots for catalysts 1 and 4 (Figure S6) are available free of charge via the Internet at <http://pubs.acs.org>.

OM0103097